hep-ph/0108268
Aug 31, 2001

Signals for Non-Commutative QED in $e\gamma$ and $\gamma\gamma$ Collisions

Stephen Godfrey
Ottawa-Carleton Institute for Physics
Department of Physics, Carleton University, Ottawa, Canada K1S 5B6

M.A. Doncheski
Department of Physics, Pennsylvania State University,
Mont Alto, PA 17237 USA

Abstract

We study the effects of non-commutative QED (NCQED) in fermion pair production, $\gamma + \gamma \to f + \bar{f}$ and Compton scattering, $e + \gamma \to e + \gamma$. Non-commutative geometries appear naturally in the context of string/M-theory and gives rise to 3- and 4-point photon vertices and to momentum dependent phase factors in QED vertices which will have observable effects in high energy collisions. We consider e^+e^- colliders with energies appropriate to the TeV Linear Collider proposals and the multi-TeV CLIC project operating in $\gamma\gamma$ and $e\gamma$ modes. Non-commutative scales roughly equal to the center of mass energy of the e^+e^- collider can be probed, with the exact value depending on the model parameters and experimental factors. However, we found that the Compton process is sensitive to Λ_{NC} values roughly twice as large as those accessible to the pair production process.

PACS numbers: 12.60.-i, 13.40.-f, 12.90.+i

I. INTRODUCTION

Although string/M-theory is still developing, and the details of its connection to the Standard Model are still unclear, numerous ideas from string/M-theory have affected the phenomenology of particle physics. The latest of these ideas is non-commutative quantum field theory (NCQFT) [1,2]. NCQFT arises through the quantization of strings by describing low energy excitations of D-branes in background EM fields. NCQFT generalizes our notion of space-time, replacing the usual, commuting, space-time coordinates with non-commuting space-time operators. This is similar to the replacement of the commuting position and momentum coordinates of classical physics with the non-commuting position and momentum operators of quantum mechanics. Significant, testable differences exist between QFT with commuting space-time coordinates and NCQFT. This article is an attempt to probe those changes.

At this time, the details of a general NCQFT model to compare to the Standard Model are just emerging [3]. However, a non-commuting replacement of quantum electrodynamics, NCQED, does exist and can be studied. NCQED modifies QED, with the addition of a non-Lorentz invariant, momentum dependent phase factor to the normal $ee\gamma$ vertex, along with the addition of cubic ($\gamma\gamma\gamma$) and quartic ($\gamma\gamma\gamma\gamma$) coupling, also, with non-Lorentz invariant momentum dependent phase factors. The Feynman rules for NCQED are given in [4,5], and will not be repeated here. Although the momentum dependent phase factors and higher dimensional operators in the Lagrangian (leading to additional couplings) arise naturally in NCQFT, the modifications, although similar, will in general, take on a different form than those presented here for NCQED. We will see that the modifications of NCQFT to QED can be probed in $\gamma\gamma \to f\bar{f}$ and $e\gamma \to e\gamma$ collisions.

The essential idea of NCQFT is that in the non-commuting space time the conventional coordinates are represented by operators which no longer commute:

$$[\hat{X}_\mu, \hat{X}_\nu] = i\theta_{\mu\nu} \equiv \frac{i}{\Lambda_{NC}^2} C_{\mu\nu} \tag{1}$$

Here we adopt the Hewett-Petriello-Rizzo parametrization [5] where the overall scale, Λ_{NC}, characterizes the threshold where non-commutative (NC) effects become relevant and $C_{\mu\nu}$ is a real antisymmetric matrix whose dimensionless elements are presumably of order unity. One might expect the scale Λ_{NC} to be of order the Planck scale. However, given the possibility of large extra dimensions [6,7] where gravity becomes strong at scales of order a TeV, it is possible that NC effects could set in at a TeV. We therefore consider the possibility that Λ_{NC} may lie not too far above the TeV scale.

The C matrix is not a tensor since its elements are identical in all reference frames resulting in the violation of Lorentz invariance. The $C_{\mu\nu}$ matrix is related to the Maxwell field strength tensor $F_{\mu\nu}$ since NCQFT arises from string theory in the presence of background electromagnetic fields. Hence, C can be parameterized, following the notation of [8], as

$$C_{\mu\nu} = \begin{pmatrix} 0 & C_{01} & C_{02} & C_{03} \\ -C_{01} & 0 & C_{12} & -C_{13} \\ -C_{02} & -C_{12} & 0 & C_{23} \\ -C_{03} & C_{13} & -C_{23} & 0 \end{pmatrix} \tag{2}$$

where $\sum_i |C_{0i}|^2 = 1$. Thus, the C_{0i} are related to space-time NC and are defined by the direction of the background **E**-field. Furthermore, the C_{0i} can be parameterized as

$$\begin{aligned} C_{01} &= \sin\alpha\cos\beta \\ C_{02} &= \sin\alpha\sin\beta \\ C_{03} &= \cos\alpha. \end{aligned} \tag{3}$$

β defines the origin of the ϕ axis which we set to $\beta = \pi/2$ and α is the angle of the background **E**-field relative to the z-axis. Likewise, the C_{ij} are related to the space-space non-commutativeness and are defined by the direction of the background **B**-field. They can be parameterized as

$$\begin{aligned} C_{12} &= \cos\gamma \\ C_{13} &= \sin\gamma\sin\beta \\ C_{23} &= -\sin\gamma\cos\beta. \end{aligned} \tag{4}$$

NCQFT can be cast in the form of conventional commuting QFT through the application of Weyl-Moyal correspondance [9]. The details of this derivation is given by Ref. [5]. The net result is that the QED vertices pick up phase factors dependent on the momenta flowing through them and three and four point photon vertices are now present. These NCQED modifications are what is being tested in collider tests of NCQED. In addition, covariant derivatives can only be constructed for (fermion) fields of charge 0, ± 1 so we restrict our analysis to processes involving only charged leptons. The Feynman rules for NCQED are given in Ref. [4,5].

NCQED is beginning to attract theoretical and phenomenological interest [5,10–12]. Hewett, Petriello and Rizzo [5] have performed a series of phenomenological studies of NC-QED at high energy, linear, e^+e^- colliders. They analyzed diphoton production ($e^+ + e^- \to \gamma + \gamma$), Bhabha scattering ($e^+ + e^- \to e^+ + e^-$) and Moller scattering ($e^- + e^- \to e^- + e^-$). There are striking differences between QED and NCQED for all three processes; most interesting is significant structure in the ϕ angular distribution.

Mathews [11] and Baek, Ghosh, He and Hwang [12] have also studied NCQED at high energy e^+e^- linear colliders. In the former case Mathews studied high energy Compton scattering while Baek *et al.,* studied fermion pair production in $\gamma + \gamma \to e^+ + e^-$. In both cases the initial state photons are due to backscattering of laser photons off the electron and positron beams. As is well known, this produces a high luminosity, high energy photon beam, effectively converting an e^+e^- collider to an $e\gamma$ or $\gamma\gamma$ collider [16]. Independently of the aforementioned studies we studied Compton scattering and lepton pair production. In our study we studied the angular distributions, in contrast to the work of Mathews [11] and Baek *et al.,* [12] whose analysis is based on the total cross section and which do not use the additional information inherent in the angular distributions. We find that the analysis based on angular distributions leads to exclusion limits on the NCQED scale of order 100 GeV or more greater than those obtained by simply measuring the total cross section. In addition we also studied the effect on sensitivity of including systematic errors in addition to statistical errors. There are a number of other differences between our work and that of these authors. In the first case, Mathews seems to have calculated the NC phase appearing in the cross section in the $e\gamma$ center of mass. This is an inherently Lorentz violating quantity and we believe that it should be to calculated in the lab frame. We therefore disagree with his approach. In the case of the work of Baek *et al.* we decided on different kinematic cuts which we feel to be more realistic. Ultimately, the best approach will be decided by experimentalists, based on detailed detector simulations. To this end, it may be of some use to see the tradeoffs inherent in different approaches.

In the following sections we will examine the effects of NCQED in $\gamma\gamma \to f\bar{f}$ and Compton scattering, $e\gamma \to e\gamma$. In the case of Compton scattering NCQED leads to an oscillatory azimuthal dependence due to the preferred direction in the laboratory frame defined by the C matrix. As will be discussed in detail later, we find that the Compton scattering process yields significantly higher exclusion limits than the pair production process, despite lower statistics.

Before proceeding we reiterate that the $C_{\mu\nu}$ matrix is not Lorentz invariant and the vectors C_{i0} and C_{ij} point in specific directions which are the same in all reference frames. In our analysis we define the z-axis to correspond to the direction of the incoming particles in the lab frame. If the experiment were to be repeated at a different location, the co-ordinates will be in general be different. In fact, as the earth rotates and revolves around the Sun, the co-ordinate system also rotates. Hence, it is important that the local co-ordinates be converted to a common frame such as a slowly varying astronomical co-ordinate system so that all measurements are made with respect to a common frame. More germaine to our specific examples is that one must calculate the cross sections in the lab frame not the centre of mass frame of either the initial $\gamma\gamma$ or $e\gamma$ beams since each event will have a different momentum fraction of the initial electron beams and hence different boosts between the lab and center of mass frames.

II. CALCULATIONS AND RESULTS

We begin by discussing the common points of our two analyses. We will present details and results from the pair production and Compton scattering prosesses in separate subsections below.

In both cases, we consider linear e^+e^- colliders operating at $\sqrt{s} = 0.5$ and 0.8 TeV appropriate to the TESLA proposal, [13] $\sqrt{s} = 0.5$, 1.0 and 1.5 TeV as advocated by the NLC proponents [14], and $\sqrt{s} = 3.0$, 5.0 and 8.0 TeV being considered in CLIC studies [15]. In order to estimate event rates, we assume an integrated luminosity of $L = 500$ fb^{-1} for all cases. We impose acceptance cuts on the final state particles of $10^o \leq \theta \leq 170^o$ and $p_T > 10\, GeV$.

As noted above, we take $\beta = \pi/2$. Therefore, in the pair production case, where only space-time NC enters, only the parameter α remains in addition to Λ_{NC}. We consider three specific cases, $\alpha = 0$, $\pi/4$ and $\pi/2$, and report limits on Λ_{NC} for each of these values. In the Compton scattering case, both space-space and space-time NC enter, leaving the two parameters, α and γ in addition to Λ_{NC}. We examine the two values $\gamma = 0$ and $\gamma = \pi/2$, and for each value of γ give exclusion limits for $\alpha = 0$, $\pi/4$ and $\pi/2$.

In order to quantify the sensitivity to NCQED, we calculate the χ^2 for the deviations between NCQED and the SM for a range of parameter values. We start by calculating statistical errors based on an integrated luminosity of 500 fb^{-1}. We assume that the statistical errors are gaussian, which given the large event rates, is certainly valid. We consider two possibilities for systematic errors. In the first case we do not include systematic errors while in the second case we obtain limits by combining a 2% systematic error combined in quadrature with the statistical errors; $\delta = \sqrt{\delta_{stat}^2 + \delta_{sys}^2}$. The 2% systematic error is a very conservative estimate of systematic errors, for example the TESLA TDR calls for only a 1% systematic error. Our exclusions limits including systematic errors should therefore be considered conservative estimates of those thought to be eventually achievable. Next, we calculate total cross sections, and $\cos\theta$ and ϕ angular distributions in both QED and NCQED. We bin the angular distributions into 20 bins in $\cos\theta$ and ϕ. Finally, we calculate the χ^2 for the different observables, $\mathcal{O}$, using:

$$\chi^2_{\mathcal{O}}(\Lambda) = \sum_i \left(\frac{\mathcal{O}_i(\Lambda) - \mathcal{O}_i^{QED}}{\delta\mathcal{O}_i} \right)^2 \tag{5}$$

where $\mathcal{O}$ represents the observable under consideration and the sum is over the bins of the angular distributions. $\chi^2 = 4$ represents a 95% C.L. deviation from QED, which we'll define as the sensitivity limit.

A. Pair Production

For the pair production process, Figure 1 shows the Feynman diagrams that contribute. Note the presence of the novel s-channel contribution from the presence in NCQED of the 3γ self-coupling. The differential cross section for this process is given by:

$$\frac{d\sigma(\gamma\gamma \to f\bar{f})}{d\cos\theta\, d\phi} = \frac{\alpha^2}{2s} \left\{ \frac{\hat{u}}{\hat{t}} + \frac{\hat{t}}{\hat{u}} - 4\frac{\hat{t}^2 + \hat{u}^2}{\hat{s}^2} \sin^2\left(\frac{k_1 \cdot \theta \cdot k_2}{2} \right) \right\}. \tag{6}$$

The first two terms in the expression are the standard QED contributions, while the last term is due to the Feynman diagram with the cubic $\gamma\gamma\gamma$ coupling. The phase factor, $\sin^2\left(\frac{k_1 \cdot \theta \cdot k_2}{2}\right)$ only appears in this new term. p_1 and p_2 are the momentum of the electron and positron, respectively, while k_1 and k_2 are the momenta of the incoming photons. $\hat{s}$, $\hat{t}$ and $\hat{u}$ are the usual Mandelstam variables $\hat{s} = (k_1 + k_2)^2$, $\hat{t} = (k_1 - p_1)^2$ and $\hat{u} = (k_1 - p_2)^2$. k_1 and k_2 are given by

$$k_1 = \frac{x_1\sqrt{s}}{2}(1, 0, 0, 1) \quad \text{and} \quad k_2 = \frac{x_2\sqrt{s}}{2}(1, 0, 0, -1) \tag{7}$$

where x_1 and x_2 are the momentum fractions of the two photons and the 4-vectors follow the convention of $k = (E, k_x, k_y, k_z)$. With this definition the bilinear product in eqn. 6 simplifies to

$$\frac{1}{2} k_1 \cdot \theta \cdot k_2 = \frac{\hat{s}}{4\Lambda_{NC}^2} C_{03}. \tag{8}$$

The expression for the cross section is not Lorentz invariant due to the presence of the phase factor. Note that only space-time non-commutativity contributes and there is no ϕ dependence in this case. In the limit $\Lambda_{NC} \to \infty$ the angle goes to zero and the SM is recovered. Given that we've chosen $\beta = \pi/2$, $C_{03} = \cos\alpha$, and the phase factor is identically zero for $\alpha = \pi/2$. Thus, for $\alpha = \pi/2$, the NCQED and QED calculations should be identical, and **no** limits on Λ_{NC} are possible for $\alpha = \pi/2$.

Fig. 2 shows the cross section for $\gamma\gamma \to e^+e^-$ vs. Λ_{NC} for QED and NCQED with $\alpha = 0$ and $\pi/4$, for a $\sqrt{s} = 0.5$ TeV e^+e^- collider operating in $\gamma\gamma$ mode. The event rate is high with statistics that can exclude NCQED to a fairly high value of Λ_{NC}. Note that the QED (solid) curve is actually a central QED value with $\pm 1\sigma$ bands (assuming 500 fb^{-1} of integrated luminosity). Fig. 3 shows the $\cos\theta$ angular distribution, $d\sigma/d\cos\theta$ for QED and NCQED with $\alpha = 0$, and $\sqrt{s} = 500\ GeV$ and $\Lambda_{NC} = 300\ GeV$.

We calculated the significance of deviations from the SM using the total cross section and by binning the angular distribution. We found that the $\cos\theta$ distribution consistently gives the highest exclusion limits on Λ_{NC}, regardless of $\sqrt{s}$ and α (as long as $\alpha \neq \pi/2$, where, again, no limits are possible).

The exclusion limits based on lepton pair production in $\gamma\gamma$ collisions and assuming an integrated luminosity of $L = 500 fb^{-1}$ are summarized in Table I for $\alpha = 0$ and $\pi/4$. These are based on the angular distribution which, as already noted, gives the highest limits. These limits could be improved by including three lepton generations in the final state and assuming some value for the lepton detection efficiency.

We also considered the limits on the NC-scale that could be obtained in e^+e^- collisions using Weizsäcker-Williams photons. Assuming 500 fb^{-1} of integrated luminosity and no systematic errors for $\sqrt{s} = 500$ GeV and 5 TeV, Λ_{NC} can be probed to 175 GeV and 370 GeV respectively for $\alpha = 0$. These limits are pretty much irrelevant compared to the limits that can be obtained in the more direct processes of Bhabba scattering and $e^+e^- \to \gamma\gamma$ in high energy e^+e^- collisions [5].

B. Compton scattering

For the Compton scattering process, Figure 4 shows the Feynman diagrams that contribute. We find:

$$\frac{d\sigma(e^-\gamma \to e^-\gamma)}{d\cos\theta\ d\phi} = \frac{\alpha^2}{2s}\left\{-\frac{\hat{u}}{\hat{s}} - \frac{\hat{s}}{\hat{u}} + 4\frac{\hat{s}^2 + \hat{u}^2}{\hat{t}^2}\sin^2\left(\frac{k_1 \cdot \theta \cdot k_2}{2}\right)\right\}. \tag{9}$$

The first two terms in the expression are the standard, QED contribution, while the last term is due to the Feynman diagram with the cubic $\gamma\gamma\gamma$ coupling. As before, the phase factor only appears in this new term.

Here, p_1 and k_1 are the momenta of the initial state electron and photon, respectively, while p_2 and k_2 are the momenta of the final state electron and photon, respectively. $\hat{s}$, $\hat{t}$ and $\hat{u}$ are the usual Mandelstam variables $\hat{s} = (p_1 + k_1)^2$, $\hat{t} = (p_1 - p_2)^2$ and $\hat{u} = (p_1 - k_2)^2$. Choosing $k_1 = x\frac{\sqrt{s}}{2}(1, 0, 0, -1)$ and $k_2 = k(1, \sin\theta\cos\phi, \sin\theta\sin\phi, \cos\theta)$, the phase factor can be evaluated analytically:

$$\frac{1}{2}k_1 \cdot \theta \cdot k_2 = \frac{xk\sqrt{s}}{4\Lambda_{NC}^2}[(C_{01} - C_{13})\sin\theta\cos\phi + (C_{02} + C_{23})\sin\theta\sin\phi + C_{03}(1 + \cos\theta)]. \tag{10}$$

where x is the momentum fraction of the incident photon, k is the magnitude of the 3-momentum of the final state photon, and θ and ϕ are the lab frame angles of the final state photon. Note that there is no C_{12} term appearing in the above expression since defining the z-axis along the beam direction results in no **B** field in the C_{12} direction. It is clear that this phase factor includes both space-space and space-time NC parts, so this process probes γ, in addition to α and β. We will again choose $\beta = \pi/2$, leaving us two free parameters in adddition to Λ_{NC}. In this case the phase factor simplifies to

$$\frac{1}{2} k_1 \cdot \theta \cdot k_2 = \frac{xk\sqrt{s}}{4\Lambda_{NC}^2}[-\sin\gamma\sin\theta\cos\phi + \sin\alpha\sin\theta\sin\phi + \cos\alpha(1+\cos\theta)]. \tag{11}$$

We remind the reader that $\alpha = 0$ corresponds to **E** parallel to the z-axis and $\alpha = \pi/2$ corresponds to **E** perpendicular to the z-axis. Because Compton scattering is sensitive to both γ and α, it is complimentary to the pair production process studied above.

After analyzing our results, the total cross section consistently gives the weakest exclusion limits on Λ_{NC}. For $\gamma = 0$, the $\cos\theta$ distribution gives the strongest exclusion limits when $\alpha = 0$ or $\pi/2$, while the ϕ distribution gives the highest exclusion limits when $\alpha = \pi/4$. For $\gamma = \pi/2$, the ϕ distribution gives the highest exclusion limits when $\alpha = 0$, while the $\cos\theta$ distribution gives the highest exclusion limits when $\alpha = \pi/4$ and $\pi/2$. When including a 2% systematic uncertainty, the ϕ distribution becomes more important: for $\gamma = 0$ the ϕ distribution gives the highest exclusion limits for $\alpha = \pi/4$ or $\pi/2$, while for $\gamma = \pi/2$, the ϕ distribution gives the highest exclusion limits for all values of α tested.

1. $\gamma = 0$ exclusion limits

Fig. 5 shows the cross section σ vs. Λ_{NC} for QED and NCQED with $\alpha = 0$, $\pi/4$ and $\pi/2$, for a $\sqrt{s} = 0.5\ TeV$ e^+e^- collider operating in $e\gamma$ mode. The event rate is high, so there are enough statistics to probe NCQED up to a fairly high value of Λ_{NC}. Again, the QED (solid) curve includes the central QED value and $\pm 1\sigma$ bands (assuming 500 fb^{-1} of integrated luminosity). Fig. 6a and Fig. 6b show the angular distributions, $d\sigma/d\cos\theta$ and $d\sigma/d\phi$, for QED and NCQED with $\alpha = \pi/2$, and $\sqrt{s} = \Lambda_{NC} = 500\ GeV$. The error bars in Fig. 6 assume 500 fb^{-1} of integrated luminosity.

Note that there is no ϕ dependence for $\alpha = 0$ since for this case both **E** and **B** are parallel to the beam direction. In contrast, when $\alpha = \pi/2$, **E** is perpendicular to the beam direction which is reflected in the strong oscillatory behavior in the ϕ distribution.

The exclusion limits obtainable from Compton scattering are summarized in Table II for $L = 500 fb^{-1}$. Limits are given for the three values of $\alpha = 0$, $\alpha = \pi/4$, and $\alpha = \pi/2$. We give the highest limits obtained from the total cross section, $d\sigma/d\cos\theta$ or $d\sigma/d\phi$. With no systematic errors the $\cos\theta$ distribution gave the best limits for $\alpha = 0$ and $\pi/2$, while the ϕ distribution gives the highest exclusion limits when $\alpha = \pi/4$. When systematic errors are included the ϕ distribution gave the best limits except for the case $\alpha = \gamma = 0$ where there is no ϕ dependence.

2. $\gamma = \pi/2$ exclusion limits

Fig. 7 shows the cross section σ vs. Λ_{NC} for QED and NCQED with $\alpha = 0$, $\pi/4$ and $\pi/2$, for a $\sqrt{s} = 0.5\ TeV$ e^+e^- collider operating in $e\gamma$ mode. Again, the QED (solid) curve includes the central QED value and $\pm 1\sigma$ bands (assuming 500 fb^{-1} of integrated luminosity). Fig. 8a and Fig. 8b show the angular distributions, $d\sigma/d\cos\theta$ and $d\sigma/d\phi$, for QED and NCQED with $\alpha = \pi/2$, and $\sqrt{s} = \Lambda_{NC} = 500\ GeV$. The error bars in Fig. 8 assume $500 fb^{-1}$ of integrated luminosity. The exclusions limits for these cases are given in Table II. With no systematic errors, when $\gamma = \pi/2$, the ϕ distribution gives the highest exclusion limits when $\alpha = 0$, while the $\cos\theta$ distribution gives the highest exclusion limits when $\alpha = \pi/4$ and $\pi/2$. When including a 2% systematic uncertainty, the ϕ distribution gives the highest exclusion limits for all values of α tested.

III. CONCLUSIONS

In conclusion, we found that lepton pair production and Compton scattering at high energy linear colliders are excellent processes to study non-commutative QED. These processes compliment those studied by Hewett, Petriello and Rizzo [5].

The pair production process is only sensitive to space-time NC and is therefore insensitive to γ. As α increases towards $\pi/2$ the deviations from SM decrease towards zero, with $\alpha = \pi/2$ being identical to the SM. On the other hand, the Compton scattering process is sensitive to both space-space and space-time NC as parametrized by γ and α. On the whole, we found that the Compton scattering process is superior to lepton pair production in probing NCQED. Despite significantly smaller statistics, the large modification of angular distributions (see Fig. 6 and 8) leads to higher exclusion limits, well in excess of the center of mass energy for all colliders considered.

After the completion of this work M. Chaichian *et al.* [3] presented a model for the NC SM. The primary implication from NCSM vs NCQED in the context of our calculations is the introduction of a $\gamma\gamma Z$ vertex. Although this will alter details of our results we do not expect it to change our main conclusions. This is the philosophy followed by Hewett *et al.* [5].

ACKNOWLEDGMENTS

The authors thank JoAnne Hewett and Tom Rizzo for many helpful conversations and communications. This research was supported in part by the Natural Sciences and Engineering Research Council of Canada. M.A.D. would like to thank the Physics Department at Carleton University where much of this work was performed.

REFERENCES

[1] For a recent review see: M. R. Douglas and N. A. Nekrasov, hep-th/0106048.

[2] A. Connes, *Non-commutative Geometry*, Academic Press, 1994; J. Gomis, M. Kleban, T. Mehen, M. Rangamani and S. Shenker, JHEP **0008**, 011 (200) [hep-th/0003215]; E. T. Akhmedov, P. DeBoer and G. W. Semenoff, hep-th/0010003; A. Rajaraman and M. Rozali, JHEP **0004**, 033 (2000) [hep-th/0003227]; J. Gomis, T. Mehen and M. B. Wise, JHEP **0008**, 029 (2000) [hep-th/0006160]; J. W. Moffat, Phys. Lett. **B491**, 345(2000) [hep-th/0007181]; F. Lizzi, G. Mangano and G. Miele, Mod. Phys. Lett. **A16**, 1 (2001) [hep-th/0009180]; J. Gomis, K. Kamimura and T. Mateos, JHEP **0103**, 010 (2001) [hep-th/0009158].

[3] M. Chaichian, P. Presnajder, M. M. Sheikh-Jabbari and A. Tureanu, hep-th/0107055.

[4] A. Armoni, Nucl. Phys. **B593**, 229 (2001) [hep-th/0005208]; M.M. Sheikh-Jabbari, J. High Energy Phys. **9906**, 015 (1999); T. Krajewski and R. Wulkenhaar, Int. J. Mod. Phys. **A15**, 1011 (2000) [hep-th/9903187]; I. Ya Aref'eva, D.M. Belov, A.S. Koshelev and O.A. Rytchkov, Nucl. Phys. Proc. Suppl. **102**, 11 (2001) [hep-th/0003176]; F. Ardalan and N. Sadooghi, Int. J. Mod. Phys. **A16** 3151 (2001) [hep-th/0002143].

[5] J. L. Hewett, F. J. Petriello and T. G. Rizzo, SLAC-PUB-8635 and `hep-ph/0010354`, unpublished.

[6] N. Arkani-Hamed, S. Dimopoulos and G. Dvali, Phys. Lett. **B429**, 263 (1998) and Phys. Rev. **D59**, 086004 (1999); I. Antoniadis, N. Arkani-Hamed, S. Dimopoulos and G. Dvali, Phys. Lett. **B436**, 257 (1998).

[7] L. Randall and R. Sundrum, Phys. Rev. Lett. **83**, 3370 (1999) and *ibid.*, 4690 (1999).

[8] J. L. Hewett, talk given at *Physics and Experiments with Future Linear e^+e^- Colliders*, Batavia Illinois 2000.

[9] See for example, Ihab. F. Riad and M.M. Sheikh-Jabbari, JHEP **0008**, 045 (2000) [hep-th/0008132].

[10] H. Arfaei and M.H. Yavartanoo, hep-th/0010244; A. Anisimov, T. Banks, M. Dine, and M. Graesser, hep-ph/0106356; C. E. Carlson, C. D. Carone and R. F. Lebed, hep-ph/0107291; H. Grosse and Y. Liao, hep-ph/0105090.

[11] P. Mathews, Phys. Rev. D **63**, 075007 (2001) [hep-ph/0011332].

[12] S. Baek, D. K. Ghosh, X.-G. He and W.-Y. P. Hwang, Phys. Rev. D **64**, 056001 (2001) [hep-ph/0103068].

[13] J. A. Aguilar-Saavedra *et al.*, hep-ph/0106315.

[14] T. Abe *et al.* [American Linear Collider Working Group Collaboration], hep-ex/0106058.

[15] R. W. Assmann *et al.*, CLIC Study Team, "A 3-TeV e^+e^- Linear Collider Based on CLIC Technology," Ed. G. Guignard CERN 2000-08.

[16] I.F. Ginzburg *et al.*, Nucl. Instrum. Methods, **205**, 47 (1983); *ibid* **219**, 5 (1984); V.I. Telnov, Nucl. Instrum. Methods, **A294**, 72 (1990); C. Akerlof, Report No. UM-HE-81-59 (1981; unpublished).

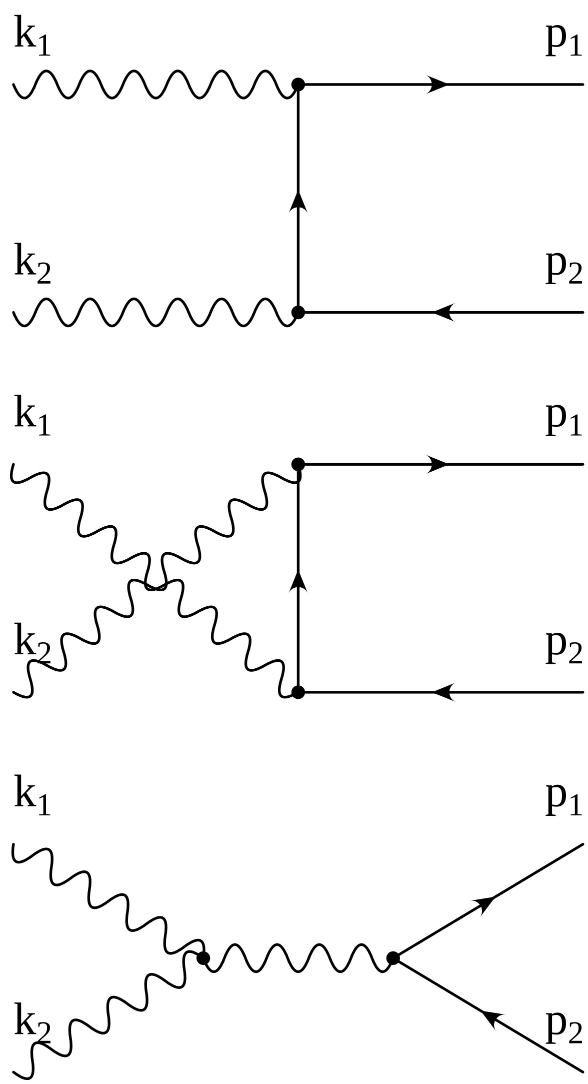

FIG. 1. The Feynman diagrams contributing to the process $\gamma\gamma \to e^+e^-$.

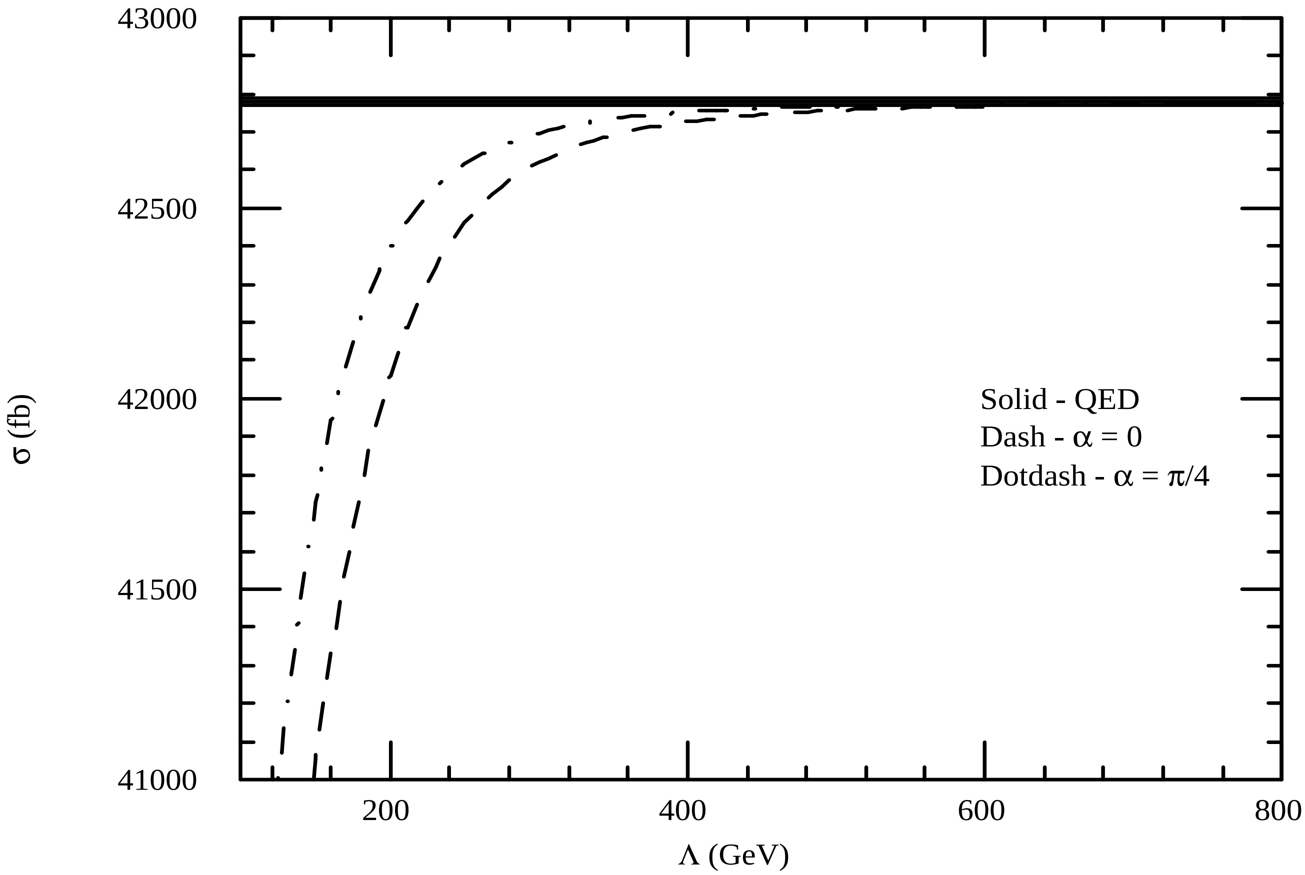

FIG. 2. σ vs. Λ_{NC} for the pair production process, $\sqrt{s} = 500$ GeV. The solid line corresponds to the SM cross section $\pm$ 1 standard deviation (statistical) error.

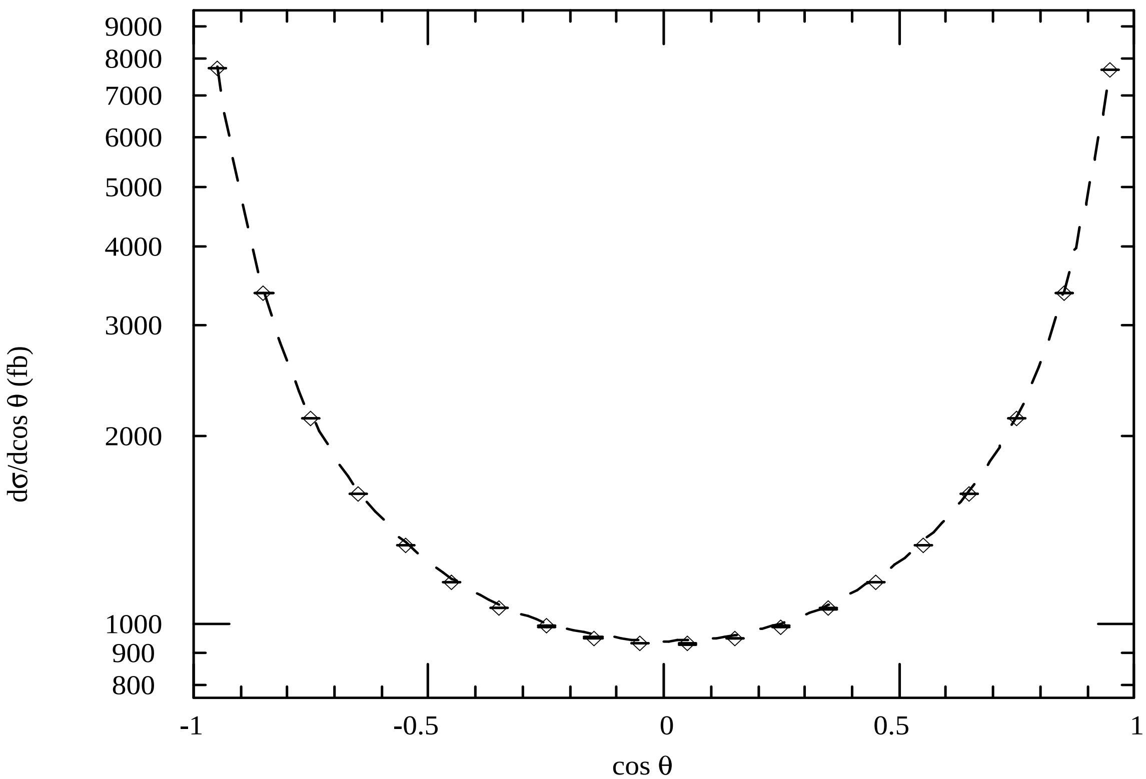

FIG. 3. $d\sigma/d\cos\theta$ vs. Λ_{NC} for the pair production process, $\sqrt{s} = 500$ GeV, $\Lambda = 300$ GeV and $\alpha = 0$. The dashed curve corresponds to the SM angular distribution and the points correspond to the NCQED angular distribution including 1 standard deviation (statistical) error.

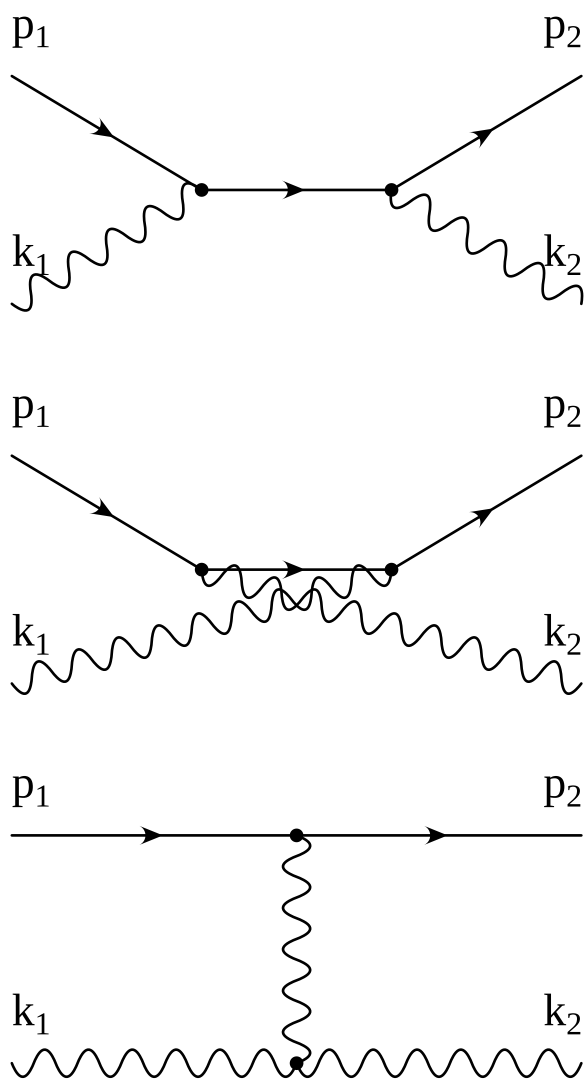

FIG. 4. The Feynman diagrams contributing to the process $e\gamma \to e\gamma$.

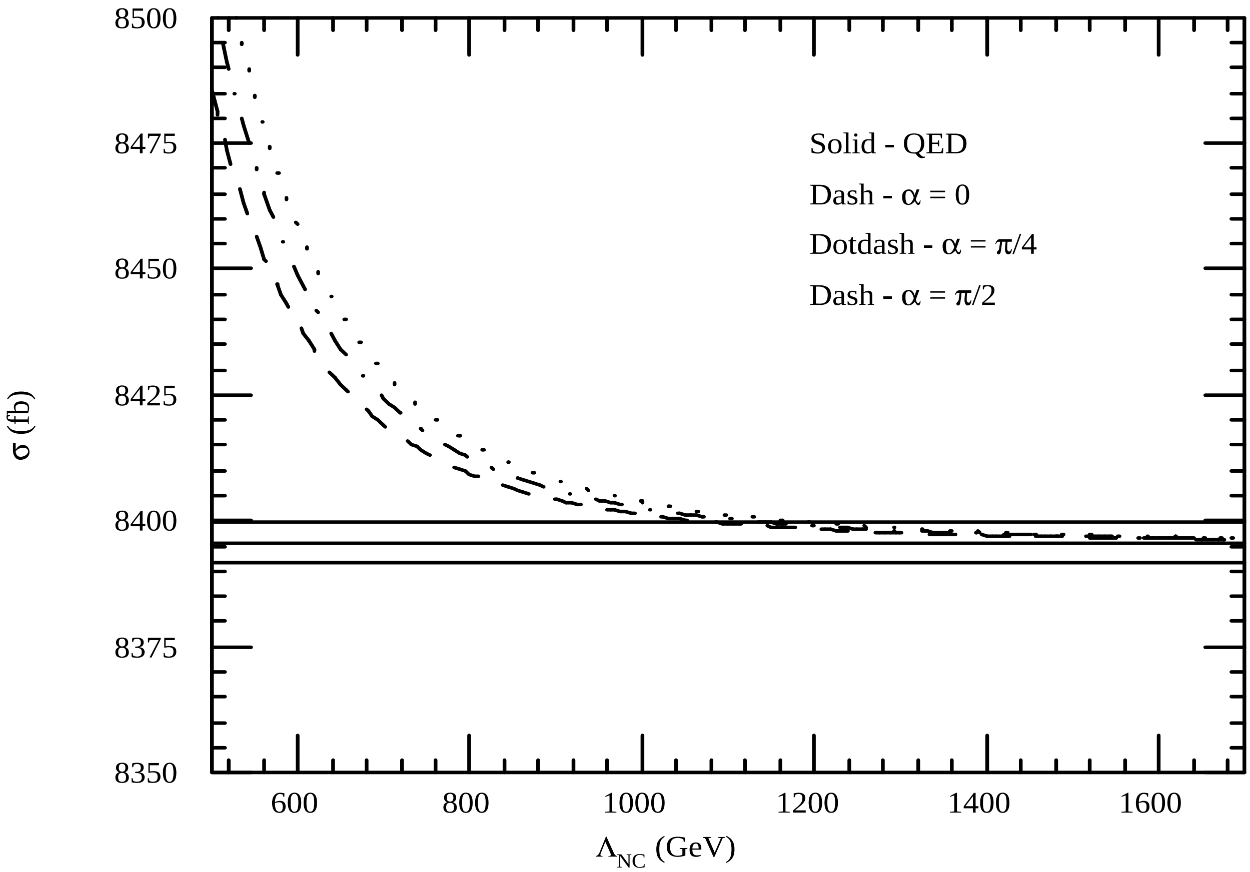

FIG. 5. σ vs. Λ_{NC} for the Compton scattering process with $\sqrt{s}$ = 500 GeV for $\gamma = 0$. The horizontal band represents the SM cross section $\pm$ 1 standard deviation (statistical) error.

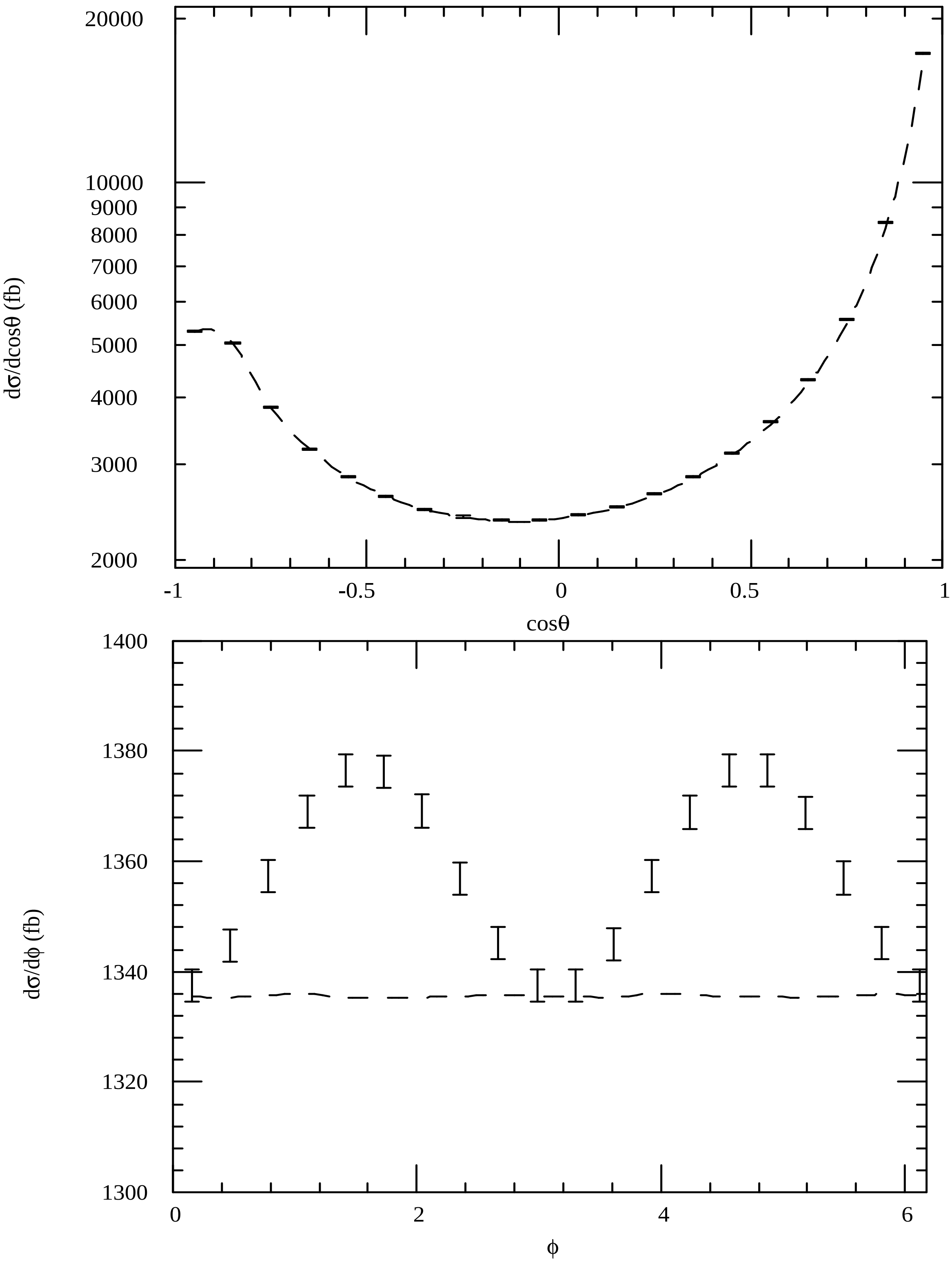

FIG. 6. (a) $d\sigma/d\cos\theta$ and (b) $d\sigma/d\phi$ for the Compton scattering process with $\sqrt{s} = 500$ GeV and for $\Lambda = 500$ GeV, $\alpha = \pi/2$ and $\gamma = 0$. The dashed curve corresponds to the SM angular distribution and the points correspond to the NCQED angular distribution including 1 standard deviation (statistical) error.

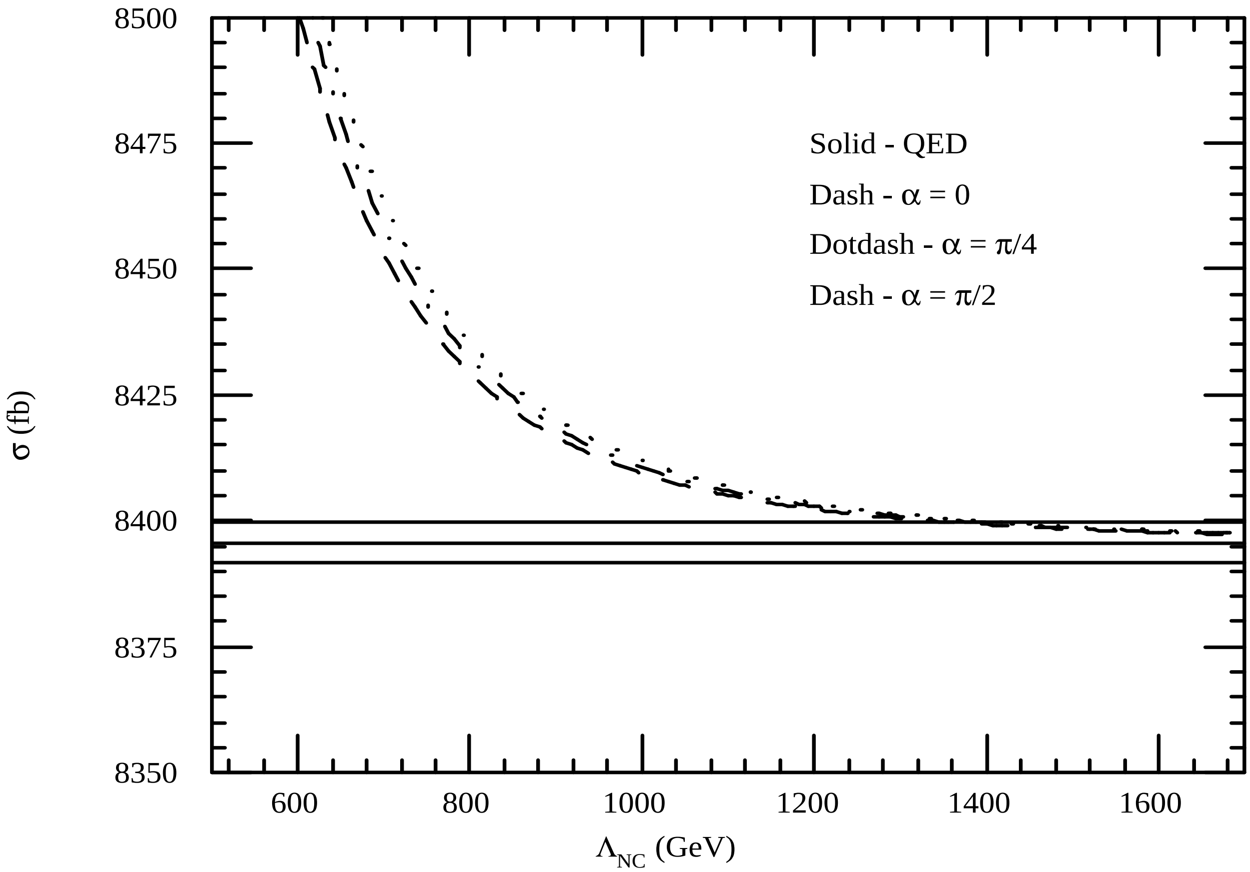

FIG. 7. σ vs. Λ_{NC} for the Compton scattering process with $\sqrt{s} = 500$ GeV for $\gamma = \pi/2$.. The horizontal band represents the SM cross section $\pm$ 1 standard deviation (statistical) error.

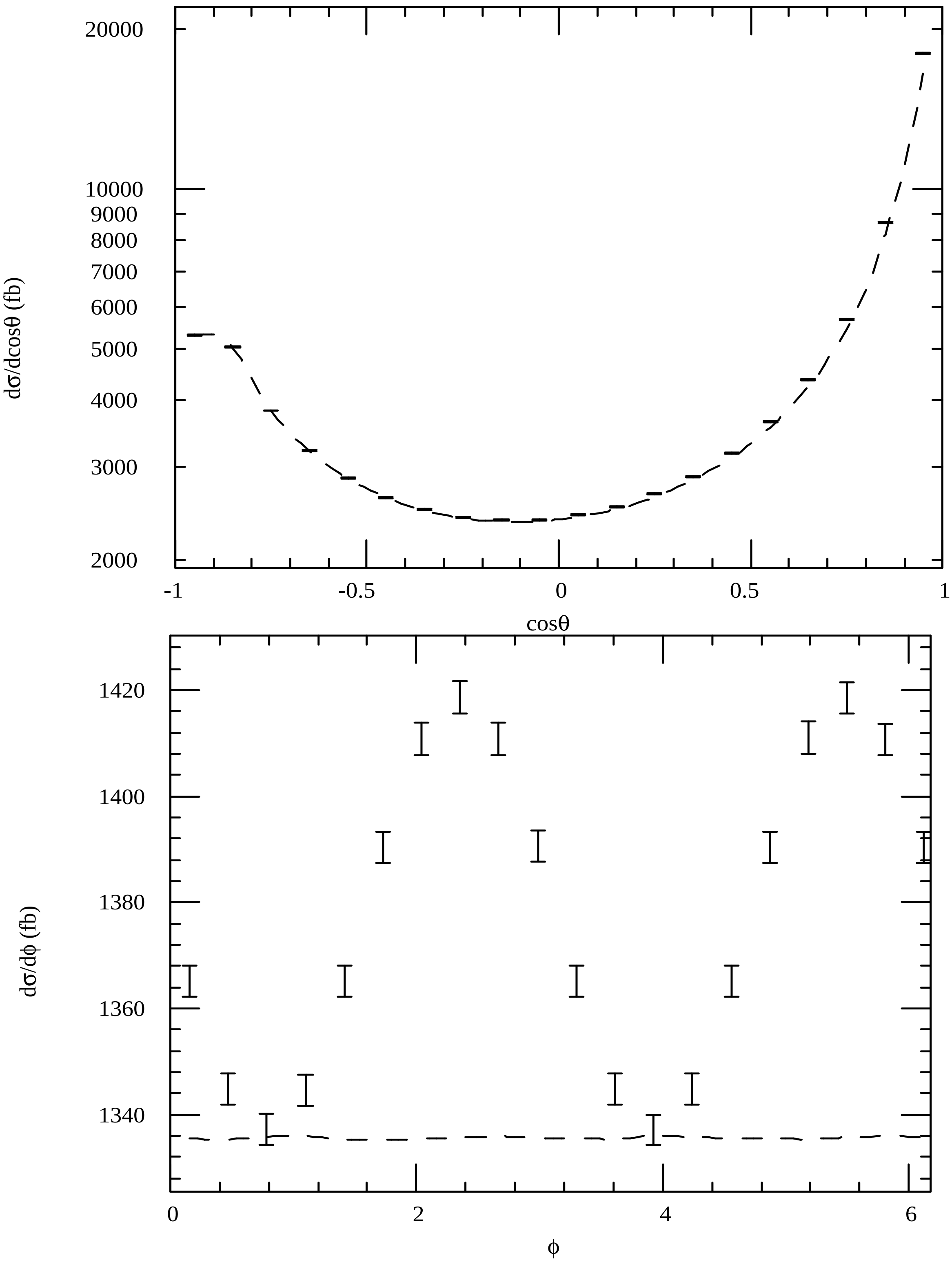

FIG. 8. (a) $d\sigma/d\cos\theta$ and (b) $d\sigma/d\phi$ for the Compton scattering process with $\sqrt{s} = 500$ GeV and for $\Lambda = 500$ GeV, $\alpha = \pi/2$ and $\gamma = \pi/2$. The dashed curve corresponds to the SM angular distribution and the points correspond to the NCQED angular distribution including 1 standard deviation (statistical) error.

TABLE I. 95% C.L. exclusion limits, in GeV, for the pair production process at a $\gamma\gamma$ collider. Results are presented for $\sqrt{s}$ = 0.5, 0.8, 1.0, 1.5, 3.0 and 5.0 TeV and for two values of α, 0 and $\pi/4$. The δ^{stat} column is with no systematic error included and the column labelled $\delta^{stat} + \delta^{sys}$ includes a 2% systematic error.

$\sqrt{s}$	$\alpha = 0$		$\alpha = \pi/4$	
(TeV)	δ^{stat}	$\delta^{stat} + \delta^{sys}$	δ^{stat}	$\delta^{stat} + \delta^{sys}$
0.5	535	260	445	220
0.8	740	400	620	335
1.0	860	485	725	405
1.5	1145	700	965	590
3.0	1880	1320	1580	1110
5.0	2700	2090	2270	1760

TABLE II. 95% C.L. exclusion limits, in GeV, for the Compton scattering process. Results are presented for $\sqrt{s}$ = 0.5, 0.8, 1.0, 1.5, 3.0 and 5.0 TeV and for $\gamma = 0$ and $\gamma = \pi/2$ and for three values of α, 0, $\pi/4$ and $\pi/2$. The δ^{stat} column is with no systematic error included and the column labelled $\delta^{stat} + \delta^{sys}$ includes a 2% systematic error.

$\sqrt{s}$ (TeV)	$\gamma = 0$					
	$\alpha = 0$		$\alpha = \pi/4$		$\alpha = \pi/2$	
	δ^{stat}	$\delta^{stat} + \delta^{sys}$	δ^{stat}	$\delta^{stat} + \delta^{sys}$	δ^{stat}	$\delta^{stat} + \delta^{sys}$
0.5	925	545	1020	585	1100	600
0.8	1325	875	1455	935	1565	960
1.0	1565	1090	1720	1165	1850	1200
1.5	2125	1620	2330	1740	2505	1785
3.0	3575	3110	3920	3375	4220	3460
5.0	5240	4880	5745	5325	6185	5465
$\sqrt{s}$ (TeV)	$\gamma = \pi/2$					
0.5	1215	700	1245	715	1305	720
0.8	1730	1115	1780	1135	1860	1140
1.0	2045	1390	2100	1415	2200	1425
1.5	2770	2070	2845	2110	2980	2125
3.0	4660	4010	4785	4085	5015	4115
5.0	6840	6335	7020	6460	7360	6500